Modern Physics Letters B
Vol. 36, Nos. 26&27 (2022) 2250146 (11 pages)

DOI: 10.1142/S0217984922501469

World Scientific
www.worldscientific.com

Higher-order localized wave solutions to a coupled fourth-order nonlinear Schrödinger equation

N. Song*,**, H. J. Shang*, Y. F. Zhang* and W. X. Ma†,‡,§,¶,††

*Department of Mathematics, North University of China, Taiyuan, Shanxi 030051, China

†Department of Mathematics, Zhejiang Normal University, Jinhua, Zhejiang 321004, China

‡Department of Mathematics, King Abdulaziz University, Jeddah 21589, Saudi Arabia

§Department of Mathematics and Statistics, University of South Florida, Tampa, FL 33620-5700, USA

¶School of Mathematical and Statistical Sciences, North-West University, Mafikeng Campus, Private Bag X2046, Mmabatho 2735, South Africa

**songni@nuc.edu.cn

††mawx@cas.usf.edu

Received 13 June 2022
Revised 27 August 2022
Accepted 14 September 2022
Published 10 December 2022

In this paper, higher-order localized waves for a coupled fourth-order nonlinear Schrödinger equation are investigated via a generalized Darboux transformation. The Nth-order localized wave solutions of this equation are derived via Lax pair and Darboux matrix. Evolution plots are made and dynamical characteristics of the obtained higher-order localized waves are analyzed through numerical simulation. It is observed that rogue waves coexist with dark–bright solitons and breathers. The presented results also show that different values of the involved parameters have diverse effects on the higher-order localized waves.

Keywords: Coupled fourth-order nonlinear Schrödinger equation; generalized Darboux transformation; localized waves.

1. Introduction

In recent years, the rapid development of optical fiber communication technology has become one of the main pillars of modern communication.[1,2] In the field

**Corresponding author.

of nonlinear optical fibers, many nonlinear phenomena can be described using nonlinear evolution equations,[3–5] which attracted more and more attention of scholars in academic researches. Due to the complexity and diversity of natural phenomena, the scholars switched their attention from single-component[6,7] to multi-component equations.[8,9] Multi-component coupled nonlinear evolution equations are used to investigate localized waves, a kind of nonlinear waves such as solitons,[10,11] breathers[12] and rogue waves.[13,14] A few methods can be applied to investigate localized waves, which include Darboux transformation (DT),[15] Bäcklund transformation,[16] the Hirota bilinear method,[17] and generalized DTs.[18–20] Localized waves in nonlinear optical fibers have been studied by many researchers, and related results provide a theoretical basis for optical fiber communications.[21–23]

In this paper, the following coupled fourth-order nonlinear Schrödinger (CNLS) equation will be studied[24–26]:

$$\begin{aligned} & iq_{j,t} + q_{j,xx} + \beta q_{j,xxxx} + 2q_j \sum_{\rho=1}^{2} |q_\rho|^2 \\ & \quad + \beta \left[2q_j \sum_{\rho=1}^{2} |q_{\rho,x}|^2 + 2q_{j,x} \sum_{\rho=1}^{2} q_\rho q_{\rho,x}^* + 6q_{j,x} \sum_{\rho=1}^{2} q_\rho^* q_{\rho,x} + 4q_{j,xx} \sum_{\rho=1}^{2} |q_\rho|^2 \right. \\ & \quad \left. + 4q_j \sum_{\rho=1}^{2} q_\rho^* q_{\rho,xx} + 2q_j \sum_{\rho=1}^{2} q_\rho q_{\rho,xx}^* + 6q_j \left(\sum_{\rho=1}^{2} |q_\rho|^2 \right)^2 \right] = 0, \quad (j = 1, 2), \end{aligned} \tag{1}$$

where $q_1(x,t)$ and $q_2(x,t)$ are the complex envelopes of the two kinds of polarization in the electric field, x and t indicate propagation distance and evolution time, respectively. The $*$ denotes complex conjugate, and the parameter β represents the strength of the higher-order linear and nonlinear effects.

There are some research results on Eq. (1). Lan displays three shapes of rogue waves via the DT.[27] The interaction among rogue waves, bright-dark solitons and breathers is discussed, and rogue waves pair is presented.[28] Four different types of breathers are considered.[29] Based on a second-order generalized DT, Wang *et al.* obtain two- and three-soliton solutions.[30]

However, there are few studies on dynamics of the third-order localized waves of Eq. (1). This paper will derive the Nth-order generalized DT on the basis of classical DT and limiting method, basic solutions will be constructed and the third-order localized wave solutions will be generated via a generalized DT.

This paper is arranged as follows. In Sec. 2, the generalized DT will be derived, and the higher-order localized wave solutions will be obtained. In Sec. 3, on the basis of numerical simulation, the evolution plots of the higher-order localized waves are given, and their dynamical characteristics are analyzed. Section 4 concludes.

2. Generalized Darboux Transformation

The following Lax pair is considered[31]:

$$\Phi_x = U\Phi, \tag{2a}$$

$$\Phi_t = V\Phi, \tag{2b}$$

where

$$U = i\lambda\sigma + P,$$

$$\begin{aligned} V = {} & 8i\beta\sigma\lambda^4 + 8\beta P\lambda^3 + [4i\beta P_x\sigma + 4i\beta P^2\sigma + 2i(I-\sigma)]\lambda^2 + (4\beta P^3 - 2\beta P_{xx} \\ & - 2\beta PP_x + 2\beta P_x P - 2P)\lambda + i\beta\sigma P_{xxx} - i\beta P_{xx}P\sigma - i\beta PP_{xx}\sigma + i\beta P_x^2\sigma \\ & + 3i\beta P^2P_x\sigma + 3i\beta P_xP^2\sigma + i\sigma P_x - i\sigma P^2 + 3i\beta\sigma P^4, \end{aligned}$$

$$\sigma = \begin{pmatrix} -1 & 0 & 0 \\ 0 & 1 & 0 \\ 0 & 0 & 1 \end{pmatrix}, \quad P = \begin{pmatrix} 0 & q_1^* & q_2^* \\ -q_1 & 0 & 0 \\ -q_2 & 0 & 0 \end{pmatrix}.$$

The Darboux matrix T is constructed as follows:

$$T = \lambda I - H\Lambda H^{-1}, \tag{3}$$

where

$$H = \begin{pmatrix} \varphi_1 & -\phi_1^* & -\chi_1^* \\ \phi_1 & \varphi_1^* & 0 \\ \chi_1 & 0 & \varphi_1^* \end{pmatrix}, \quad \Lambda = \begin{pmatrix} \lambda_1 & 0 & 0 \\ 0 & \lambda_1^* & 0 \\ 0 & 0 & \lambda_1^* \end{pmatrix}.$$

$\Phi = (\varphi_1, \phi_1, \chi_1)^T$ is the eigenfunction of Eq. (2) corresponding to the spectral parameter $\lambda = \lambda_1$ and seed solutions $q_1 = q_1[0]$ and $q_2 = q_2[0]$. The DT of Eq. (1) is obtained from the Darboux matrix T as follows:

$$\lambda = \lambda_k, \quad \Phi_k = (\varphi_k, \phi_k, \chi_k)^T, \quad (k = 1, 2, \ldots, N), \tag{4}$$

$$\Phi_N[N-1] = T[N-1]T[N-2]\ldots T[1]\Phi_N, \tag{5}$$

$$q_1[N] = q_1[0] - 2i\sum_{k=1}^{N}(\lambda_1 - \lambda_1^*)\frac{\varphi_k^*[k-1]\phi_k[k-1]}{|\varphi_k[k-1]|^2 + |\phi_k[k-1]|^2 + |\chi_k[k-1]|^2}, \tag{6a}$$

$$q_2[N] = q_2[0] - 2i\sum_{k=1}^{N}(\lambda_1 - \lambda_1^*)\frac{\varphi_k^*[k-1]\chi_k[k-1]}{|\varphi_k[k-1]|^2 + |\phi_k[k-1]|^2 + |\chi_k[k-1]|^2}, \tag{6b}$$

where

$$T[k] = \lambda_{k+1}I - H[k-1]\Lambda[k]H[k-1]^{-1},$$

$$\Phi_k[k-1] = (T[k-1]T[k-2]\cdots T[1])|_{\lambda=\lambda_k}\Phi_k,$$

$$H[k-1]=\begin{pmatrix}\varphi_k[k-1] & -\phi_k^*[k-1] & -\chi_k^*[k-1]\\ \phi_k[k-1] & \varphi_k^*[k-1] & 0\\ \chi_k[k-1] & 0 & \varphi_k^*[k-1]\end{pmatrix},$$

$$\Lambda[k]=\begin{pmatrix}\lambda_k & 0 & 0\\ 0 & \lambda_k^* & 0\\ 0 & 0 & \lambda_k^*\end{pmatrix}.$$

Based on the above classical DT, a generalized DT of Eq. (1) is constructed. Assuming $\Phi_1=\Phi_1(\lambda_1,\eta)$ is a solution of Eq. (2) and η is a small parameter, Taylor expansion of Φ_1 at $\eta=0$ is obtained as follows:

$$\Phi_1=\Phi_1^{[0]}+\Phi_1^{[1]}\eta+\Phi_1^{[2]}\eta^2+\cdots+\Phi_1^{[N]}\eta^N+o(\eta^N), \tag{7}$$

where

$$\Phi_1^{[k]}=\frac{1}{k!}\frac{\partial^k}{\partial\lambda^k}\Phi_1(\lambda)|_{\lambda=\lambda_1}=(\varphi_1^{[k]},\phi_1^{[k]},\chi_1^{[k]})^T,\quad (k=0,1,2,\ldots,N).$$

It is easy to verify that $\Phi_1^{[0]}=\Phi_1[0]$ is a special solution with $\lambda=\lambda_1$, $q_1=q_1[0]$ and $q_2=q_2[0]$ of Eq. (2). Thus, the generalized DT is defined as follows:

$$\begin{aligned}\Phi_1[N-1]=\Phi_1^{[0]}&+\left[\sum_{l=1}^{N-1}T_1[l]\right]\Phi_1^{[1]}+\left[\sum_{l=1}^{N-1}\sum_{h>l}^{N-1}T_1[h]T_1[l]\right]\Phi_1^{[2]}\\&+\cdots+[T_1[N-1]\ldots T_1[2]T_1[1]]\Phi_1^{[N-1]},\end{aligned} \tag{8}$$

$$\begin{aligned}q_1[N]&=q_1[N-1]\\&\quad-2i(\lambda_1-\lambda_1^*)\frac{\varphi_1^*[N-1]\phi_1[N-1]}{|\varphi_1[N-1]|^2+|\phi_1[N-1]|^2+|\chi_1[N-1]|^2},\end{aligned} \tag{9a}$$

$$\begin{aligned}q_2[N]&=q_2[N-1]\\&\quad-2i(\lambda_1-\lambda_1^*)\frac{\varphi_1^*[N-1]\chi_1[N-1]}{|\varphi_1[N-1]|^2+|\phi_1[N-1]|^2+|\chi_1[N-1]|^2},\end{aligned} \tag{9b}$$

where

$$T_1[k]=\lambda_1 I-H_1[k-1]\Lambda_1 H_1[k-1]^{-1},$$

$$\Phi_1[N-1]=(\varphi_1[N-1],\phi_1[N-1],\chi_1[N-1])^T,$$

$$H_1[k-1]=\begin{pmatrix}\varphi_1[k-1] & -\phi_1^*[k-1] & -\chi_1^*[k-1]\\ \phi_1[k-1] & \varphi_1^*[k-1] & 0\\ \chi_1[k-1] & 0 & \varphi_1^*[k-1]\end{pmatrix},$$

$$\Lambda_1 = \begin{pmatrix} \lambda_1 & 0 & 0 \\ 0 & \lambda_1^* & 0 \\ 0 & 0 & \lambda_1^* \end{pmatrix}.$$

3. Dynamics of Higher-Order Localized Waves

Assuming $q_1[0] = a_1 e^{i\theta}$ and $q_2[0] = a_2 e^{i\theta}$ are seed solutions of Eq. (1), where

$$\theta = \mu x + \omega t,$$
$$\omega = -\mu^2 + 2(a_1^2 + a_2^2) + \beta[6(a_1^2 + a_2^2)^2 - 12\mu^2(a_1^2 + a_2^2) + \mu^4],$$

a_1, a_2 and μ are arbitrary real constants.

The first- and second-order localized wave solutions with $\mu = 0$ have been studied.[28] The dynamical characteristics of the higher-order localized waves will be discussed with $\mu \neq 0$ which is different from Ref. 28.

The corresponding basic vector solution at $\lambda = (\frac{\mu}{2} + i\sqrt{a_1^2 + a_2^2})(1 + \eta^2)$ is

$$\Phi_1(\eta) = \begin{pmatrix} (h_1 e^{\kappa_1 + \kappa_2} - h_2 e^{\kappa_1 - \kappa_2}) e^{-\frac{i\theta}{2}} \\ \upsilon_1 (h_1 e^{\kappa_1 - \kappa_2} - h_2 e^{\kappa_1 + \kappa_2}) e^{\frac{i\theta}{2}} + \gamma a_2 e^{\kappa_3} \\ \upsilon_2 (h_1 e^{\kappa_1 - \kappa_2} - h_2 e^{\kappa_1 + \kappa_2}) e^{\frac{i\theta}{2}} - \gamma a_1 e^{\kappa_3} \end{pmatrix}, \tag{10}$$

where

$$h_1 = \frac{\left(-\sqrt{\left(\frac{\mu}{2} - \lambda\right)^2 + (a_1\upsilon_1 + a_2\upsilon_2)^2} - \frac{\mu}{2} + \lambda\right)^{\frac{1}{2}}}{\sqrt{\left(\frac{\mu}{2} - \lambda\right)^2 + (a_1\upsilon_1 + a_2\upsilon_2)^2}},$$

$$h_2 = \frac{\left(\sqrt{\left(\frac{\mu}{2} - \lambda\right)^2 + (a_1\upsilon_1 + a_2\upsilon_2)^2} - \frac{\mu}{2} + \lambda\right)^{\frac{1}{2}}}{\sqrt{\left(\frac{\mu}{2} - \lambda\right)^2 + (a_1\upsilon_1 + a_2\upsilon_2)^2}},$$

$$\kappa_1 = 2i[(-a_1^2 - a_2^2 + \mu\lambda - 2\lambda^2)\mu^2\beta + \lambda^2]t,$$

$$\kappa_2 = i\sqrt{\left(\frac{\mu}{2} - \lambda\right)^2 + (a_1\upsilon_1 + a_2\upsilon_2)^2}(x - \tau t + \Omega(\eta)), \quad \kappa_3 = i\lambda(x + 8\beta\lambda^3),$$

$$\tau = \mu + 2\lambda + \beta[\mu(-\mu^2 + 2\mu\lambda - 4\lambda^2) + (6\mu + 4\lambda)(a_1^2 + a_2^2) - 8\lambda^3],$$

$$\upsilon_1 = \frac{a_1}{\sqrt{a_1^2 + a_2^2}}, \quad \upsilon_2 = \frac{a_2}{\sqrt{a_1^2 + a_2^2}}, \quad \Omega(\eta) = \sum_{j=1}^{N} (m_j + in_j)\eta^{2j}, \quad (m_j, n_j \in R),$$

α_j, m_j and n_j are arbitrary real constants. Let $\delta = a_1^2 + a_2^2$, and expand function $\Phi_1(\eta)$ be Taylor series at $\eta = 0$,

$$\Phi_1(\eta) = \Phi_1^{[0]} + \Phi_1^{[1]}\eta^2 + \Phi_1^{[2]}\eta^4 + \Phi_1^{[3]}\eta^6 + \cdots, \tag{11}$$

where

$$\Phi_1(\eta) = (\varphi_1^{[k]}, \phi_1^{[k]}, \chi_1^{[k]})^T = \frac{1}{(2k)!}\frac{\partial^{2k}\Phi_1}{\partial\eta^{2k}}|_{\eta=0}, \quad (k = 0, 1, 2, \ldots),$$

$$\begin{aligned}
\varphi_1^{[0]} &= \delta^{-\frac{1}{4}}\left(\frac{\sqrt{2}}{2} + \frac{\sqrt{2}}{2}i\right)[2ix\delta^{\frac{1}{2}} + i + 4\delta t + 24\beta\delta^2 t \\
&\quad - 4i\delta^{\frac{1}{2}}\mu t(1 + 12\beta\delta) + 4\beta\delta^{\frac{1}{2}}\mu^2 t(i\mu - 4\delta^{\frac{1}{2}})]e^{\zeta_1}, \\
\phi_1^{[0]} &= -\delta^{-\frac{3}{4}}\left(\frac{\sqrt{2}}{2} + \frac{\sqrt{2}}{2}i\right)a_1[2i\delta^{\frac{1}{2}}x + 24\beta\delta^2 t + 4\delta t - i \\
&\quad - 4i\delta^{\frac{1}{2}}\mu t(12\beta\delta + 1) + 4\beta\delta^{\frac{1}{2}}\mu^2 t(i\mu - 4\delta^{\frac{1}{2}})]e^{\zeta_2} + \gamma a_2 e^{\zeta_3}, \\
\chi_1^{[0]} &= -\delta^{-\frac{3}{4}}\left(\frac{\sqrt{2}}{2} + \frac{\sqrt{2}}{2}i\right)a_2[2i\delta^{\frac{1}{2}}x + 24\beta\delta^2 t + 4\delta t - i \\
&\quad - 4i\delta^{\frac{1}{2}}\mu t(12\beta\delta + 1) + 4\beta\delta^{\frac{1}{2}}\mu^2 t(i\mu - 4\delta^{\frac{1}{2}})]e^{\zeta_2} - \gamma a_1 e^{\zeta_3}, \\
\zeta_1 &= 2\mu t(\mu^2\beta - 1)\delta^{\frac{1}{2}} + \frac{-i\mu x + \mu^2 t(-i\beta\mu^2 + 16i\delta\beta + 2i) - 6i\delta t(\delta\beta + 1)}{2}, \\
\zeta_2 &= 2\mu t(\mu^2\beta - 1)\delta^{\frac{1}{2}} + \frac{i\mu x + i\beta\mu^2 t(\mu^2 - 8\delta) + 2i\delta t(3\beta\delta - 1)}{2}, \\
\zeta_3 &= [i\delta^{-\frac{1}{2}}x + 8\beta\delta t - 12i\beta\delta^{\frac{1}{2}}\mu t + \beta\mu^2 t(i\delta^{-\frac{1}{2}}\mu - 6)]\left(i\delta + \frac{\mu}{2}\delta^{\frac{1}{2}}\right).
\end{aligned}$$

Owing to the expression $\Phi_1^{[j]} = (\varphi_1^{[j]}, \phi_1^{[j]}, \chi_1^{[j]})^T$ $(j = 1, 2)$ which is complicated, its specific form is omitted.

Based on the following limit formula:

$$\begin{aligned}
\Phi_1[2] &= \lim_{\eta\to 0}\frac{T[2]|_{\lambda=\lambda_1(1+\eta^2)}T[1]|_{\lambda=\lambda_1(1+\eta^2)}\Phi_1}{\eta^4} \\
&= \lim_{\eta\to 0}\frac{(\lambda_1\eta^2 + T_1[2]|_{\lambda=\lambda_1})(\lambda_1\eta^2 + T_1[1]|_{\lambda=\lambda_1})\Phi_1}{\eta^4} \\
&= \lambda_1^2\Phi_1^{[0]} + \lambda_1(T_1[2] + T_1[1])\Phi_1^{[1]} + (T_1[2]T_1[1])\Phi_1^{[2]}, \qquad (12)
\end{aligned}$$

and Eqs. (8) and (9), the third-order localized wave solutions can be obtained

$$q_1[3] = q_1[2] - 2i(\lambda_1 - \lambda_1^*)\frac{\varphi_1^*[2]\phi_1[2]}{|\varphi_1[2]|^2 + |\phi_1[2]|^2 + |\chi_1[2]|^2}, \qquad (13a)$$

$$q_2[3] = q_2[2] - 2i(\lambda_1 - \lambda_1^*)\frac{\varphi_1^*[2]\chi_1[2]}{|\varphi_1[2]|^2 + |\phi_1[2]|^2 + |\chi_1[2]|^2}, \qquad (13b)$$

where

$$\Phi_1[2] = (\varphi_1^{[2]}, \phi_1^{[2]}, \chi_1^{[2]}),$$

$$T_1[1] = \lambda_1 I - H_1[0]\Lambda_1 H_1[0]^{-1},$$
$$T_1[2] = \lambda_1 I - H_1[1]\Lambda_1 H_1[1]^{-1},$$
$$H_1[0] = \begin{pmatrix} \varphi_1[0] & -\phi_1^*[0] & -\chi_1^*[0] \\ \phi_1[0] & \varphi_1^*[0] & 0 \\ \chi_1[0] & 0 & \varphi_1^*[0] \end{pmatrix},$$
$$H_1[1] = \begin{pmatrix} \varphi_1[1] & -\phi_1^*[1] & -\chi_1^*[1] \\ \phi_1[1] & \varphi_1^*[1] & 0 \\ \chi_1[1] & 0 & \varphi_1^*[1] \end{pmatrix},$$
$$\Lambda_1 = \begin{pmatrix} \lambda_1 & 0 & 0 \\ 0 & \lambda_1^* & 0 \\ 0 & 0 & \lambda_1^* \end{pmatrix}.$$

The evolution plots of different third-order localized waves are obtained by altering the values of the free parameters. Next, the dynamics of third-order localized wave solutions are discussed in different cases.

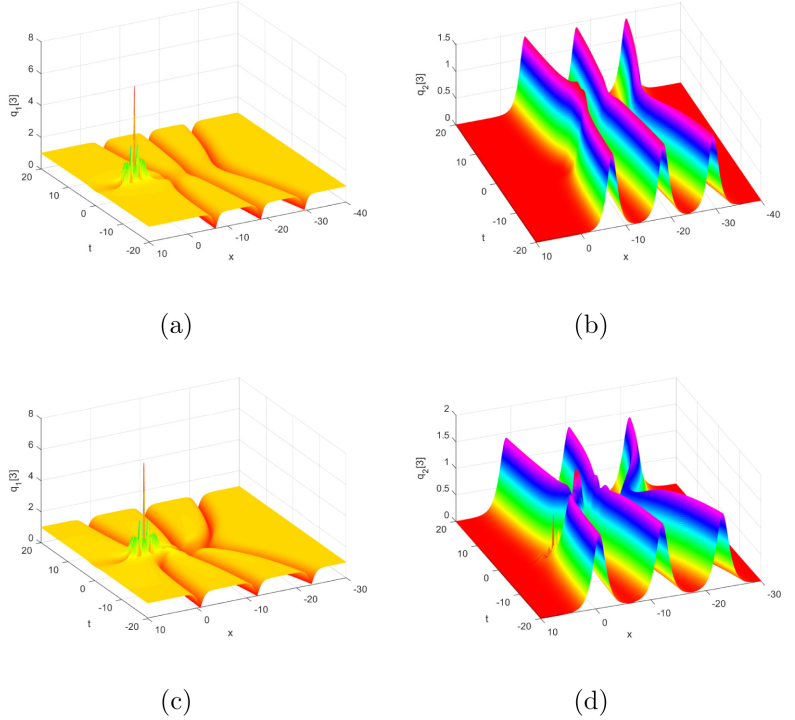

Fig. 1. (Color online) The third-order localized waves with $a_1 = 1, a_2 = m_1 = m_2 = n_1 = n_2 = 0, \mu = \frac{1}{100}$, $\beta = \frac{1}{10}$ and (a) $\gamma = \frac{1}{5000}$; (b) $\gamma = \frac{1}{5000}$; (c) $\gamma = \frac{1}{10}$; (d) $\gamma = \frac{1}{10}$.

Case 1. $\mu = \gamma = 0$, $a_1 \neq 0$, $a_2 \neq 0$ and $\beta \neq 0$.

Let $m_1 = m_2 = n_1 = n_2 = 0$, $q_1[3]$ and $q_2[3]$ be the basic third-order rogue waves, and their amplitude is maximum at the center. Let $m_1 = m_2 = n_1 = n_2 \neq 0$, the third-order rogue waves are separated into six first-order rogue waves. The evolution plots of third-order rogue waves are omitted in this paper.

Case 2. $\mu \neq 0$, $a_1 \neq 0$, and $a_2 = 0$.

Let $m_1 = m_2 = n_1 = n_2 = 0$, the interaction between third-order rogue waves and three dark solitons can be obtained in Fig. 1(a). As shown in Fig. 1(b), the third-order rogue waves in the component $q_2[3]$ are not easily observed in the background of zero amplitude. It can be seen that the third-order rogue waves are merged with the three dark solitons by increasing the value of γ in Fig. 1(c).

Let $m_1 = m_2 = n_1 = n_2 \neq 0$, it is obvious that the third-order rogue waves in the component $q_1[3]$ are separated into six first-order rogue waves in Fig. 2(a). Similarly, as seen in Fig. 2(b), it is difficult to observe rogue waves in the component $q_2[3]$. Moreover, Figs. 2(c) and 2(d) exhibit the change of the propagation direction of bright–dark solitons by altering the value of μ.

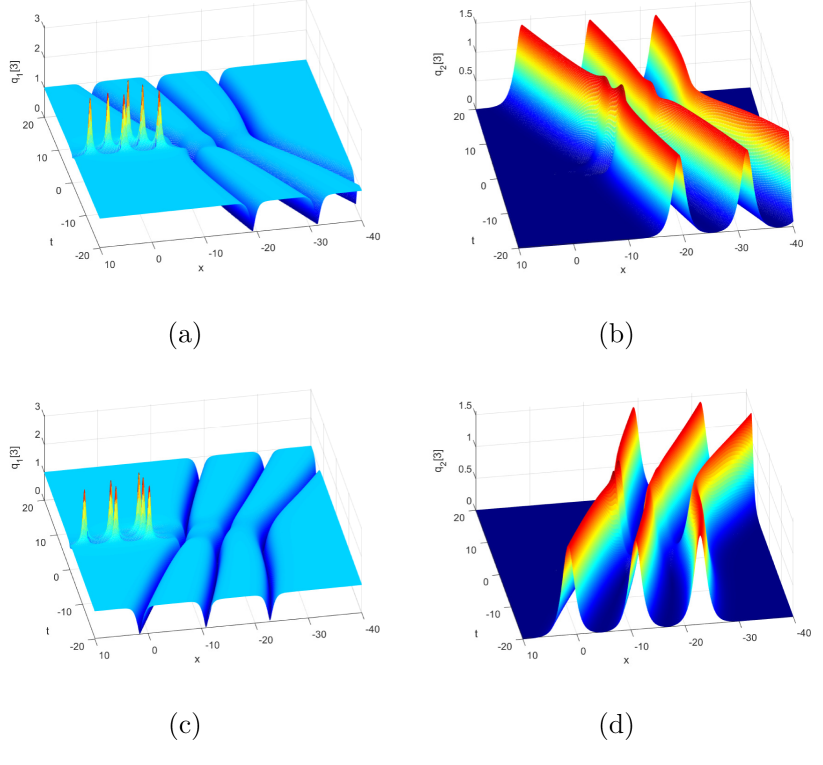

Fig. 2. (Color online) The third-order localized waves with $a_1 = 1, a_2 = 0, m_1 = m_2 = n_1 = n_2 = 30, \gamma = \frac{1}{100000}, \beta = \frac{1}{5}$ and (a) $\mu = \frac{1}{10}$; (b) $\mu = \frac{1}{10}$; (c) $\mu = -\frac{1}{10}$; (d) $\mu = -\frac{1}{10}$.

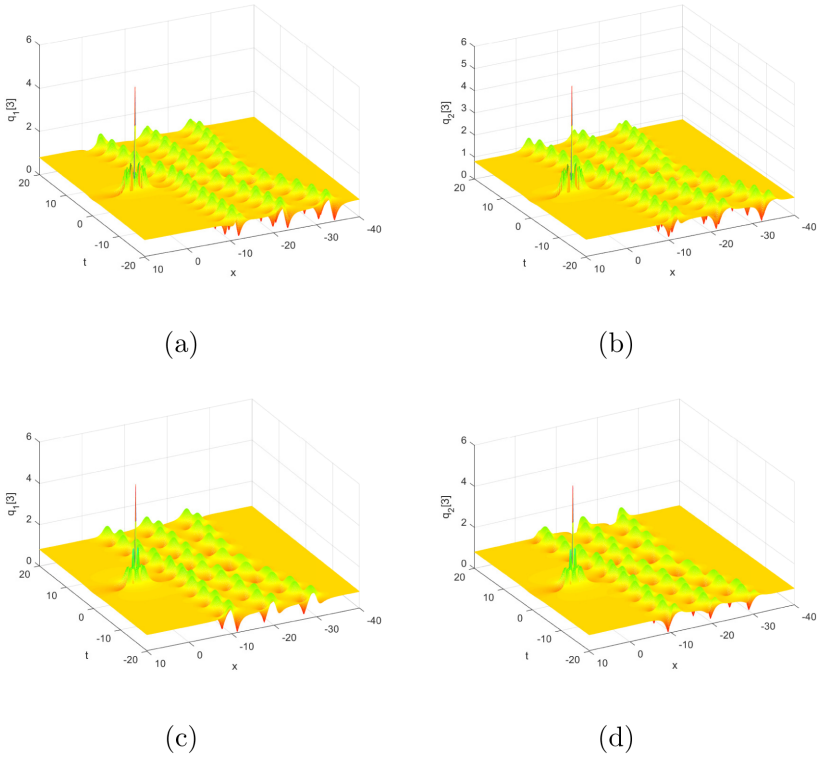

Fig. 3. (Color online) The third-order localized waves with $a_1 = a_2 = \frac{4}{5}, m_1 = m_2 = n_1 = n_2 = 0, \mu = \frac{1}{20}$, $\gamma = \frac{1}{100000}$ and (a) $\beta = \frac{1}{10}$; (b) $\beta = \frac{1}{10}$; (c) $\beta = \frac{1}{100}$; (d) $\beta = \frac{1}{100}$.

Cases 3. $\mu \neq 0, a_1 \neq 0$ and $a_2 \neq 0$.

Let $m_1 = m_2 = n_1 = n_2 = 0$, Figs. 3(a) and 3(b) display the interaction between the third-order rogue waves and three breathers, and the dynamic characteristics of the components $q_1[3]$ and $q_2[3]$ are basically consistent. On decreasing the value of β, Figs. 3(c) and 3(d) show that the three breathers' period increases.

Let $m_1 = m_2 = n_1 = n_2 \neq 0$, due to the separation function, the third-order rogue waves appear as a separation phenomenon and interact with the three breathers, as shown in Figs. 4(a) and 4(b).

In summary, the parameters have an important influence on the dynamics of the localized waves.

The parameters a_1 and a_2 influence the type of localized waves. If $a_1 \neq 0$ and $a_2 = 0$, the third-order rogue waves interact with three dark–bright solitons. If $a_1 \neq 0$ and $a_2 \neq 0$, it is observed that the third-order rogue waves coexist with three breathers.

The parameters m_j, n_j, $(j = 1, 2)$ play an important role in the separation of third-order rogue waves. When the parameters m_j, n_j are not equal to 0, the third-order rogue waves can be separated into six first-order rogue waves.

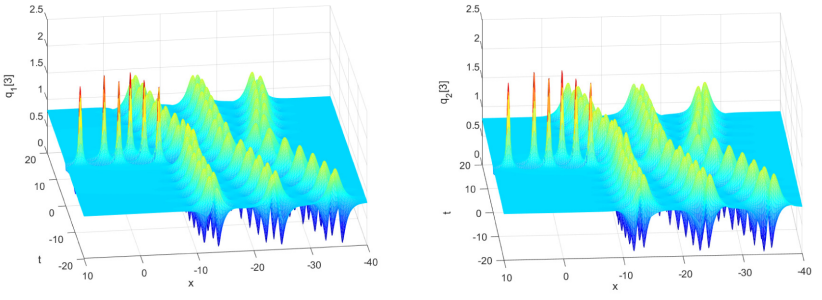

(a) (b)

Fig. 4. (Color online) The third-order localized waves with $a_1 = a_2 = \frac{4}{5}, \mu = \frac{1}{20}, \gamma = \frac{1}{500000}, \beta = \frac{1}{10}$ and (a) $m_1 = m_2 = n_1 = n_2 = 50$; (b) $m_1 = m_2 = n_1 = n_2 = 50$.

The parameter μ has an important influence on the propagation direction of three dark–bright solitons and breathers. As $\mu < 0$, the included angle between the propagation direction of the three dark–bright solitons or breathers and the positive direction of t-axis is an obtuse angle, or else is an acute angle.

The parameter γ leads to the separation of the third-order rogue waves from the three dark–bright solitons and breathers. As the parameter γ increases, the third-order rogue waves gradually merge the three dark-bright solitons and breathers.

The parameter β determines the period and spacing of the three dark–bright solitons and breathers. As β decreases, the period of the three breathers increases.

4. Conclusions

On the basis of seed solutions and the Lax pair, a coupled fourth-order nonlinear Schrödinger equation was studied by a generalized DT. Dynamical characteristics of the localized waves were analyzed by altering the values of the involved parameters, including the interaction between higher-order rogue waves and dark–bright solitons or breathers. The obtained results enrich dynamics of localized waves in a birefringent optical fiber.

Acknowledgments

The authors sincerely would like to thank the support of the National Natural Science Foundation of China (NNSFC) through Grant No. 11602232, the Graduate Innovation Project Fund of Shanxi Province through Grant No. 2021Y629, and Research Project Supported by Shanxi Scholarship Council of China through Grant No. 2022-150. Fundamental Research Program of Shanxi Province through Grant No. 202203021211086.

References

1. G. P. Agrawal, *Nonlinear Fiber Optics*, 3rd edn, Lecture Notes in Physics, Vol. 18, (2001), p. 195.
2. D. Iida, N. Honda and H. Oshida, *Opt. Fiber Technol.* **57** (2020) 102263.
3. X. F. Wu, G. S. Hua and Ma, *Nonlinear Dyn.* **70** (2012) 2259.
4. X. Lu and B. Tian, *Nonlinear Anal.: Real World Appl.* **14** (2013) 929.
5. A. Biswas *et al.*, *Optik* **142** (2017) 73.
6. Z. Zhou, J. Fu and Z. Li, *Appl. Math. Comput.* **217** (2010) 92.
7. Z. Alizadeh and H. Panahi, *Ann. Phys.* **409** (2019) 167920.
8. X. S. Xiang and D. W. Zuo, *Optik* **241** (2021) 167061.
9. Y. Zhai, T. Ji and X. Geng, *Appl. Math. Comput.* **411** (2021) 126551.
10. M. Tahir, A. U. Awan and H. ur Rehman, *Optik* **199** (2019) 163297.
11. E. M. E. Zayed, R. M. A. Shohib and M. E. M. Alngar, *Optik* **243** (2021) 167406.
12. Z. Z. Lan, *Appl. Math. Lett.* **102** (2020) 106132.
13. S. L. Jia, Y. T. Gao and L. Hu, *Optik* **142** (2017) 90.
14. B. Q. Li and Y. L. Ma, *Optik* **174** (2018) 178.
15. D. Y. Liu and H. M. Yu, *Appl. Math. Lett.* **118** (2021) 107154.
16. Y. Yang, T. Suzuki and J. Wang, *Commun. Nonlinear Sci. Numer. Simul.* **95** (2021) 105626.
17. Y. Yue, L. Huang and Y. Chen, *Appl. Math. Lett.* **89** (2019) 70.
18. T. Xu and Y. Chen, *Chin. Phys. B* **25** (2016) 090201.
19. N. Song, H. Xue and Y. K. Xue, *Commun. Nonlinear Sci. Numer. Simul.* **82** (2020) 105046.
20. N. Song, X. Y. Zhao and N. Shi, *Int. J. Dyn. Control* **9**(2021) 1396.
21. H. P. Chai, B. Tian and Z. Du, *Commun. Nonlinear Sci. Numer. Simul.* **70** (2019) 181.
22. X. W. Yan, *Appl. Math. Lett.* **107** (2020) 106414.
23. D. Y. Yang *et al.*, *Chaos, Solitons Fractals* **150** (2021) 110487.
24. D. Y. Liu, B. Tian and X. Y. Xie, *Mod. Phys. Lett. B* **31** (2017) 1750067.
25. W. R. Sun, D. Y. Liu and X. Y. Xie, *Chaos* **27** (2017) 043114.
26. Z. Zhang *et al.*, *Eur. Phys. J. Plus* **134** (2019) 1.
27. Z. Z. Lan, *Appl. Math. Lett.* **98** (2019) 128.
28. T. Xu and G. L. He, *Nonlinear Dyn.* **98** (2019) 1731.
29. Z. Du *et al.*, *Chaos Solitons Fractals* **130** (2020) 109403.
30. M. Wang *et al.*, *Appl. Math. Lett.* **119** (2021) 106936.
31. W. X. Ma, *Nonlinear Anal. Real World Appl.* **47** (2019) 1.